Research Square

Preprints are preliminary reports that have not undergone peer review.
They should not be considered conclusive, used to inform clinical practice,
or referenced by the media as validated information.

Joint profiles of remnant cholesterol and the uric acid-to-HDL cholesterol ratio in transitions across cardiovascular-diabetes-kidney multimorbidity and death

Yihan Wang
Guangdong Medical University
Haipeng Wang
Guangdong Medical University
Yiyan Li
Guangdong Medical University
Xitong Xu
Guangdong Medical University
Qian Liu
Guangdong Medical University
Songwen Liu
Guangdong Medical University
Chen Li
Guangdong Medical University
ruoxuan wang
Guangdong Medical University
xin zhang
Guangdong Medical University
Yuqing He
yuqing.he@gdmu.edu.cn
Guangdong Medical University

Research Article

Keywords: remnant cholesterol, uric acid-to-HDL cholesterol ratio, multimorbidity, cardiovascular-kidney-metabolic health, multi-state model, CHARLS

Posted Date: November 18th, 2026

DOI: https://doi.org/10.21203/rs.3.rs-10984633/v1

License: This work is licensed under a Creative Commons Attribution 4.0 International License.
Read Full License

Additional Declarations: No competing interests reported.

Abstract

Background

The accumulation of cardiovascular, diabetes, and kidney conditions is a dynamic public-health process. Remnant cholesterol (RC) and the uric acid-to-high-density lipoprotein cholesterol ratio (UHR) are readily available metabolic markers, yet little is known about how their combined levels relate to progression through successive multimorbidity states.

Methods

We included 10,560 CHARLS participants with valid baseline RC, UHR, age, observed disease state, and linked mortality status. Four joint RC/UHR profiles were examined using a covariate-adjusted discrete-time Markov model to estimate destination-specific relative risk ratios across the multimorbidity pathway. Benjamini-Hochberg adjustment was applied to the 27 prespecified profile tests. Continuous exposure, RC-quality, and cut-point analyses assessed robustness. A separate HRS analysis was placed in the Supplement as supportive external context because its biomarkers and disease-state definitions were not directly equivalent to CHARLS.

Results

Across 36,210 observed interval pairs from 10,343 participants, 1,269 deaths were flagged by 2020. Compared with the low RC/low UHR profile, the high RC/high UHR profile was associated with transition from no disease domain to one domain (RRR 1.245, 95% CI 1.101–1.407; BH q = 0.006) and from one domain to multimorbidity (RRR 1.437, 95% CI 1.184–1.745; BH q = 0.006). The estimate for one domain to death was higher but did not remain below 0.05 after multiplicity adjustment (RRR 1.518, 95% CI 1.079–2.134; nominal P = 0.017; BH q = 0.114). Excluding 190 participants with negative calculated RC values produced similar estimates for the two main transitions. Median-cutpoint analyses showed the same directions but were not significant after BH adjustment (q = 0.140 and q = 0.207). The continuous RC-by-UHR interaction was not clearly associated with progression.

Conclusion

In this longitudinal cohort, the joint high RC/high UHR profile identified participants more likely to enter a first cardiovascular, diabetes, or kidney disease domain and then progress to multimorbidity. The study demonstrates the value of a stage-specific multi-state framework for revealing heterogeneity that is hidden by a single multimorbidity endpoint. The findings are intended to guide further prevention and replication research, not to define causal effects or clinical thresholds.

Background

Multimorbidity is common in ageing populations. As conditions accumulate, care becomes more complicated and the risk of death rises [1–8]. The cardiovascular-kidney-metabolic framework brings adiposity, dyslipidemia, diabetes, cardiovascular disease, and kidney disease together through their shared pathways [1]. Following how people move between disease states over time may therefore reveal patterns that a single incident-disease endpoint misses.

RC is the cholesterol carried in triglyceride-rich remnant particles and has been linked to atherosclerotic disease in observational, genetic, and clinical studies [9–15]. Uric acid and HDL cholesterol reflect partly different metabolic pathways. The UHR has been associated with metabolic syndrome, kidney disease, cardiovascular disease, and mortality, although the strength and direction of these associations vary across populations [16–23]. Kidney disease is also closely linked to cardiovascular events and mortality [24, 25].

Multi-state models are designed to describe movement among clinically meaningful health states, including progression, apparent recovery-like reclassification, and death as an absorbing state [26–29]. In panel surveys, however, disease-domain states may be affected by diagnosis, access to care, treatment, recall, and missingness. Hidden Markov models can be used as a measurement-error sensitivity framework, although latent states require explicit assumptions and should not be treated as independently validated clinical diagnoses [30, 31]. By following participants across successive observed states, a multi-state model can show whether a metabolic profile is associated with different stages of disease accumulation rather than only with a single composite endpoint.

We therefore examined whether baseline RC/UHR profiles were associated with stage-specific transitions among no disease domain, one disease domain, multimorbidity, and death in CHARLS. The central innovation was to treat multimorbidity as a sequence of transitions rather than a single endpoint, allowing the association of the joint metabolic profile to be located along the disease-accumulation pathway. A separate HRS analysis was prespecified as supportive external context and is reported in Supplementary Table S7; CHARLS remains the primary analytic cohort because HRS does not provide directly comparable RC, UHR, and kidney-domain measures [3].

Methods

Study population and data sources

We conducted a longitudinal observational analysis using data from the China Health and Retirement Longitudinal Study (CHARLS) and linked mortality records from follow-up waves. CHARLS follows middle-aged and older adults in China [2]. The analysis began with 17,708 wave-1 records. We retained participants with valid baseline RC, UHR, age, baseline disease state, and a matched mortality-status record.

Exposure definitions

We calculated RC as total cholesterol minus HDL cholesterol minus LDL cholesterol, and UHR as uric acid divided by HDL cholesterol. Both measures were standardized using the mean and standard deviation of the main analytic cohort. Using the cohort mean as the cut point, we classified participants as low RC/low UHR, high RC/low UHR, low RC/high UHR, or high RC/high UHR. The low RC/low UHR profile served as the reference. A separate continuous model included standardized RC, standardized UHR, and their product interaction.

Disease states and death

We defined three disease domains: cardiovascular disease (heart disease or stroke), diabetes, and kidney disease. We then collapsed the domain count into no disease domain, one disease domain, or two or more domains (multimorbidity). Death was assigned as a fourth absorbing state at the first follow-up wave with a recorded death. Because exact participant-level death dates were unavailable, the analysis estimates transitions observed over survey intervals and cumulative death status by 2020 rather than exact-time hazards.

Primary Markov model

We created adjacent state pairs from the 2011, 2013, 2015, 2018, and 2020 CHARLS waves. For each current non-death state, a multinomial destination model estimated destination-specific relative risk ratios, using the current state as the reference destination. Models adjusted for age, sex, rural residence, body mass index, education, smoking, drinking, and calendar interval. Participant-clustered sandwich covariance accounted for repeated intervals. We retained reverse observed transitions instead of treating them as impossible, and treated death as absorbing when calculating predicted occupancy[26–29].

Multiplicity and sensitivity analyses

The primary joint-profile analysis generated 27 profile-by-destination tests: three non-reference profiles for each non-death current state and each eligible destination. We calculated Benjamini-Hochberg q values across these 27 tests. We also fitted the continuous RC/UHR interaction model. Because some calculated RC values were negative, we repeated the profile analysis after excluding participants with RC < 0 and restandardizing the exposures within the sensitivity cohort. Finally, we repeated the analysis using the cohort median rather than the cohort mean as the RC and UHR cut point.

Study Population

Figure 1 presents the assembly of the CHARLS analytic cohort. Among the 17,708 participants in the wave-1 survey, 7,148 were excluded because of missing or invalid remnant cholesterol (RC) or uric acid-to-high-density lipoprotein cholesterol ratio (UHR), age outside the prespecified range of 45–110 years or missing age, an unresolved baseline disease state, or the absence of a matched mortality-status record. This process yielded 10,560 participants meeting the primary eligibility criteria. After restricting the sample to participants with complete covariate information for the adjusted Markov models, a further 1,614 participants were excluded, resulting in a complete-case Markov cohort of 8,946 participants. Within this cohort, 6,975 participants had no disease domain at baseline (78.0%), 1,661 had a single disease domain (18.6%), and 310 had multimorbidity involving at least two disease domains (3.5%). In the longitudinal analysis, 10,343 participants from the primary baseline cohort contributed at least one observed transition, generating 36,210 adjacent interval pairs, and 1,269 deaths were identified through the 2020 mortality follow-up.

Statistical Analysis

Baseline characteristics were summarized according to baseline disease-domain status, including no disease domain, a single disease domain, and multimorbidity involving two or more domains. Remnant cholesterol (RC) was calculated as total cholesterol minus high-density lipoprotein cholesterol and low-density lipoprotein cholesterol, and the uric acid-to-high-density lipoprotein cholesterol ratio (UHR) was calculated as uric acid divided by high-density lipoprotein cholesterol. RC and UHR were standardized using cohort-specific means and standard deviations and were cross-classified into four joint profiles according to the standardized cut-point of zero: low RC + low UHR, high RC + low UHR, low RC + high UHR, and high RC + high UHR. The low RC + low UHR profile was used as the reference category.

The longitudinal disease process was represented by four observed states: no disease domain, one disease domain, multimorbidity, and death. Adjacent state transitions were evaluated across the 2011–2013, 2013–2015, 2015–2018, and 2018–2020 intervals. For each non-death current state, multinomial logistic transition models were fitted to estimate destination-specific relative risk ratios (RRRs) for progression to another disease state or death, with remaining in the current state used as the within-model reference destination. The primary models were adjusted for age, sex, rural residence, body mass index, smoking status, alcohol-use status, educational attainment, and calendar interval. Robust sandwich standard errors clustered at the participant level were used to account for the repeated observations contributed by the same individual. RRRs, 95% confidence intervals (CIs), and two-sided P values were reported. To account for multiple testing, Benjamini–Hochberg-adjusted Q values were calculated across the 27 joint-profile transition tests.

Several sensitivity analyses were performed. First, RC and UHR were modeled as continuous standardized variables, including their product interaction term, to assess the robustness of the joint-profile findings. Second, analyses were repeated after excluding participants with calculated negative RC values. Third, the joint-profile classification was repeated using cohort-specific median cut-points. Model-predicted transition probabilities were propagated across successive observation intervals to

estimate disease-state occupancy trajectories by RC/UHR profile. A constrained hidden Markov model was additionally fitted as a secondary measurement-error sensitivity analysis, with death treated as an absorbing state. Because exact dates of death were unavailable, mortality was assigned at the first available mortality-status wave, and the analyses were interpreted as interval-based state-transition analyses rather than exact-time survival analyses. All primary adjusted analyses used complete cases for the required model covariates, and no imputed values were introduced.

Secondary analyses

HRS was analysed separately as a supplementary external comparison. It provided non-HDL cholesterol rather than directly comparable RC and UHR measures and did not include a comparable kidney domain, so we did not pool HRS with CHARLS or present it as a formal replication of the Markov model [3]. The HRS estimates are reported transparently in Supplementary Table S7 and were not included in the primary multiplicity-controlled inference. The constrained hidden Markov model remained a separate measurement-error sensitivity analysis.

Primary adjusted models used complete cases for the required covariates. Multiple imputation was not undertaken because a complete harmonized missingness codebook was not available; complete-case analysis can reduce precision or introduce selection bias [33–35, 37]. Reporting was guided by the STROBE recommendations [32]. We did not replace the observed-data estimates with E-value-style or other causal sensitivity claims [36, 38].

Results

Baseline Characteristics

Baseline characteristics according to baseline disease-domain status are presented in Table 1. Among the 10,560 CHARLS participants in the baseline cohort, 8,185 (77.5%) had no observed disease domain, 1,979 (18.7%) had one disease domain, and 396 (3.8%) had multimorbidity involving at least two disease domains. Baseline age and BMI tended to be higher as disease burden increased. Mean age was 58.9, 60.7, and 61.0 years, and mean BMI was 23.3, 24.2, and 25.2 kg/m² among participants with no disease domain, one disease domain, and multimorbidity, respectively.

Table 1
Baseline characteristics by baseline multimorbidity status.

Characteristic	Overall (N = 10,560)	No disease domain (N = 8,185)	Single disease domain (N = 1,979)	Multimorbidity (> = 2 domains) (N = 396)
Participants, n	10,560	8,185	1,979	396
Age, years	59.3 (9.4)	58.9 (9.4)	60.7 (9.1)	61.0 (8.6)
Female sex, n (%)	4,966 (47.0%)	3,917 (47.9%)	882 (44.6%)	167 (42.2%)
Rural residence, n (%)	6,798 (64.4%)	5,417 (66.2%)	1,179 (59.6%)	202 (51.0%)
Education category 1, n (%) (missing n = 12)	5,025 (47.6%)	3,926 (48.0%)	919 (46.5%)	180 (45.6%)
Education category 2, n (%) (missing n = 12)	2,271 (21.5%)	1,727 (21.1%)	453 (22.9%)	91 (23.0%)
Education category 3, n (%) (missing n = 12)	2,135 (20.2%)	1,673 (20.5%)	392 (19.8%)	70 (17.7%)
Education category 4, n (%) (missing n = 12)	1,117 (10.6%)	850 (10.4%)	213 (10.8%)	54 (13.7%)
Body mass index, kg/m2 (missing n = 1,600)	23.5 (3.9)	23.3 (3.8)	24.2 (4.3)	25.2 (4.2)
Ever smoking, n (%) (missing n = 4)	4,147 (39.3%)	3,249 (39.7%)	744 (37.6%)	154 (38.9%)
Ever alcohol use, n (%) (missing n = 13)	4,121 (39.1%)	3,257 (39.8%)	722 (36.5%)	142 (35.9%)
Diabetes, n (%)	659 (6.2%)	0 (0.0%)	425 (21.5%)	234 (59.1%)
Heart disease, n (%) (missing n = 2)	1,307 (12.4%)	0 (0.0%)	989 (50.0%)	318 (80.3%)
Stroke, n (%) (missing n = 4)	286 (2.7%)	0 (0.0%)	221 (11.2%)	65 (16.4%)
Kidney disease, n (%)	618 (5.9%)	0 (0.0%)	394 (19.9%)	224 (56.6%)
Total cholesterol, mg/dL	193.29 (38.28)	192.63 (37.76)	195.22 (39.96)	197.33 (39.95)
HDL cholesterol, mg/dL	51.04 (15.32)	51.68 (15.25)	49.10 (15.34)	47.34 (15.52)
LDL cholesterol, mg/dL	116.39 (34.93)	116.01 (34.47)	117.58 (36.45)	118.28 (36.69)

Characteristic	Overall (N = 10,560)	No disease domain (N = 8,185)	Single disease domain (N = 1,979)	Multimorbidity (> = 2 domains) (N = 396)
Uric acid, mg/dL	4.47 (1.25)	4.45 (1.23)	4.53 (1.31)	4.50 (1.33)
Remnant cholesterol, mg/dL	25.86 (24.83)	24.93 (23.60)	28.53 (27.70)	31.72 (31.77)
UHR, ratio	0.097 (0.047)	0.095 (0.045)	0.103 (0.054)	0.107 (0.054)
Low RC / low UHR profile, n (%)	4,847 (45.9%)	3,885 (47.5%)	816 (41.2%)	146 (36.9%)
High RC / low UHR profile, n (%)	1,472 (13.9%)	1,132 (13.8%)	279 (14.1%)	61 (15.4%)
Low RC / high UHR profile, n (%)	1,907 (18.1%)	1,462 (17.9%)	366 (18.5%)	79 (19.9%)
High RC / high UHR profile, n (%)	2,334 (22.1%)	1,706 (20.8%)	518 (26.2%)	110 (27.8%)

Continuous variables are presented as mean (SD); categorical variables as n (%). Percentages use the non-missing denominator within each column; missing counts are shown in the characteristic label. Single disease domain denotes exactly one of the cardiovascular, diabetes, or kidney domains; multimorbidity denotes at least two domains. Education reflects the supplied harmonized categories 1-4. Baseline states do not represent irreversible biological stages.

Women and rural residents made up a smaller share of the groups with greater baseline disease burden. The proportion of women was 47.9% in the no-domain group, 44.6% in the one-domain group, and 42.2% in the multimorbidity group. The corresponding proportions of rural residents were 66.2%, 59.6%, and 51.0%.

Several metabolic markers also followed a graded pattern across baseline disease groups. Mean total cholesterol was 192.63, 195.22, and 197.33 mg/dL, while mean LDL-C was 116.01, 117.58, and 118.28 mg/dL. In contrast, mean HDL-C was 51.68, 49.10, and 47.34 mg/dL. Mean RC was 24.93, 28.53, and 31.72 mg/dL, and mean UHR was 0.095, 0.103, and 0.107. Uric acid did not show a clear monotonic pattern.

Among participants with one disease domain, heart disease, diabetes, kidney disease, and stroke were present in 50.0%, 21.5%, 19.9%, and 11.2%, respectively. The corresponding proportions among participants with multimorbidity were 80.3%, 59.1%, 56.6%, and 16.4%.

The high RC/high UHR profile was more common among participants with greater baseline disease burden: 20.8% in the no-domain group, 26.2% in the one-domain group, and 27.8% in the multimorbidity group. In contrast, the low RC/low UHR profile decreased from 47.5% to 41.2% and 36.9%.

Observed transition structure

Table 2 summarizes 36,210 adjacent state pairs across four follow-up intervals. During 2011–2013, most participants remained in the same observed state: 94.7% of those with no disease domain and 94.4% of those with one disease domain remained stable, while forward progression occurred in 5.3% and 5.6%, respectively. No deaths or reverse transitions were recorded during this interval, and all participants with multimorbidity remained in that state. During 2013–2015, the proportions remaining in the same state were 86.5% for participants with no disease domain, 83.8% for those with one disease domain, and 95.8% for those with multimorbidity; death accounted for 2.7%, 4.5%, and 4.2%, respectively. During 2015–2018, retention was lower, particularly among participants with one disease domain, of whom 61.9% remained in the same state. Reverse transitions were observed among participants with one disease domain (17.2%) and multimorbidity (22.0%), while forward progression from no disease domain occurred in 18.1%. During 2018–2020, the proportions remaining in the same state were 85.1%, 71.6%, and 74.9% among participants with no disease domain, one disease domain, and multimorbidity, respectively. Reverse transitions remained present in the one-domain and multimorbidity groups (12.5% and 18.7%), and death accounted for 3.1%, 4.5%, and 6.4%, respectively.

Table 2
Observed adjacent state pairs by interval and current state.

Interval	Current state	All pairs	Remain	Reverse	Forward progression	Death
2011–2013	No disease domain	7,502	7,106 (94.7%)	0 (0.0%)	396 (5.3%)	0 (0.0%)
2011–2013	One disease domain	1,862	1,757 (94.4%)	0 (0.0%)	105 (5.6%)	0 (0.0%)
2011–2013	Multimorbidity	364	364 (100.0%)	0 (0.0%)	0 (0.0%)	0 (0.0%)
2013–2015	No disease domain	6,626	5,733 (86.5%)	0 (0.0%)	713 (10.8%)	180 (2.7%)
2013–2015	One disease domain	1,991	1,668 (83.8%)	0 (0.0%)	233 (11.7%)	90 (4.5%)
2013–2015	Multimorbidity	451	432 (95.8%)	0 (0.0%)	0 (0.0%)	19 (4.2%)
2015–2018	No disease domain	5,848	4,528 (77.4%)	0 (0.0%)	1,061 (18.1%)	259 (4.4%)
2015–2018	One disease domain	2,294	1,419 (61.9%)	394 (17.2%)	332 (14.5%)	149 (6.5%)
2015–2018	Multimorbidity	706	480 (68.0%)	155 (22.0%)	0 (0.0%)	71 (10.1%)
2018–2020	No disease domain	5,051	4,299 (85.1%)	0 (0.0%)	593 (11.7%)	159 (3.1%)
2018–2020	One disease domain	2,561	1,833 (71.6%)	319 (12.5%)	293 (11.4%)	116 (4.5%)
2018–2020	Multimorbidity	954	715 (74.9%)	178 (18.7%)	0 (0.0%)	61 (6.4%)

Primary joint-profile Markov model

The clearest and most consistent pattern involved the high RC/high UHR profile. Compared with low RC/low UHR, high RC/high UHR was associated with transition from no disease domain to one disease domain (RRR 1.245, 95% CI 1.101–1.407; BH q = 0.006) and from one disease domain to multimorbidity (RRR 1.437, 95% CI 1.184–1.745; BH q = 0.006). High RC/low UHR was also associated with no disease domain to one disease domain (RRR 1.168, 95% CI 1.017–1.341; nominal P = 0.028), but this association did not remain below 0.05 after the 27-test adjustment (Table 3).

Table 3
Adjusted destination-specific relative risk ratios for joint RC/UHR profiles.

Current -> destination	Profile	RRR (95% CI)	Nominal P	BH q	Events
No disease domain -> One disease domain	High RC / low UHR	1.168 (1.017–1.341)	0.028	0.153	2,131
No disease domain -> One disease domain	Low RC / high UHR	0.929 (0.810–1.065)	0.290	0.490	2,131
No disease domain -> One disease domain	High RC / high UHR	1.245 (1.101–1.407)	< 0.001	0.006	2,131
No disease domain -> Multimorbidity	High RC / low UHR	1.235 (0.836–1.825)	0.290	0.490	226
No disease domain -> Multimorbidity	Low RC / high UHR	0.773 (0.506–1.183)	0.237	0.490	226
No disease domain -> Multimorbidity	High RC / high UHR	1.376 (0.982–1.930)	0.064	0.287	226
No disease domain -> Death	High RC / low UHR	1.013 (0.747–1.374)	0.932	0.934	505
No disease domain -> Death	Low RC / high UHR	1.186 (0.931–1.510)	0.167	0.427	505
No disease domain -> Death	High RC / high UHR	1.095 (0.837–1.434)	0.508	0.730	505
One disease domain -> No disease domain	High RC / low UHR	0.805 (0.616–1.051)	0.111	0.427	616
One disease domain -> No disease domain	Low RC / high UHR	0.710 (0.537–0.940)	0.017	0.114	616
One disease domain -> No disease domain	High RC / high UHR	0.838 (0.649–1.081)	0.173	0.427	616
One disease domain -> Multimorbidity	High RC / low UHR	1.058 (0.840–1.331)	0.632	0.776	816
One disease domain -> Multimorbidity	Low RC / high UHR	1.053 (0.836–1.325)	0.661	0.776	816
One disease domain -> Multimorbidity	High RC / high UHR	1.437 (1.184–1.745)	< 0.001	0.006	816
One disease domain -> Death	High RC / low UHR	1.250 (0.862–1.811)	0.239	0.490	303
One disease domain -> Death	Low RC / high UHR	1.015 (0.714–1.442)	0.934	0.934	303

Current -> destination	Profile	RRR (95% CI)	Nominal P	BH q	Events
One disease domain -> Death	High RC / high UHR	1.518 (1.079–2.134)	0.017	0.114	303
Multimorbidity -> No disease domain	High RC / low UHR	0.813 (0.338–1.958)	0.644	0.776	53
Multimorbidity -> No disease domain	Low RC / high UHR	0.611 (0.246–1.518)	0.289	0.490	53
Multimorbidity -> No disease domain	High RC / high UHR	0.682 (0.325–1.429)	0.310	0.493	53
Multimorbidity -> One disease domain	High RC / low UHR	0.862 (0.551–1.348)	0.514	0.730	224
Multimorbidity -> One disease domain	Low RC / high UHR	0.881 (0.557–1.392)	0.586	0.776	224
Multimorbidity -> One disease domain	High RC / high UHR	0.978 (0.665–1.439)	0.911	0.934	224
Multimorbidity -> Death	High RC / low UHR	0.963 (0.463-2.000)	0.919	0.934	130
Multimorbidity -> Death	Low RC / high UHR	1.482 (0.841–2.613)	0.174	0.427	130
Multimorbidity -> Death	High RC / high UHR	1.468 (0.878–2.455)	0.143	0.427	130

The high RC/high UHR estimate for one-domain to death was elevated (RRR 1.518, 95% CI 1.079–2.134; nominal P = 0.017), but its BH q value was 0.114. We therefore treat this as an exploratory nominal association rather than a multiplicity-robust positive finding. Estimates originating from multimorbidity were generally imprecise, with confidence intervals that included the null.

Multiplicity and negative-RC sensitivity analysis

The baseline cohort included 190 participants with calculated RC < 0 (1.8%). After excluding these participants, 10,370 remained. The high RC/high UHR associations with no disease domain to one disease domain and one disease domain to multimorbidity were similar in magnitude and remained below the BH-adjusted 0.05 threshold. The results of the sensitivity analysis excluding participants with calculated RC values below zero are summarized in Table 4.

Table 4
Core findings and sensitivity analysis excluding calculated RC < 0.

Transition	Profile	Main RRR (95% CI)	Main BH q	RC > = 0 RRR (95% CI)	Sensitivity BH q
No disease domain -> One disease domain	High RC / high UHR	1.245 (1.101–1.407)	0.006	1.258 (1.111–1.424)	0.004
One disease domain -> Multimorbidity	High RC / high UHR	1.437 (1.184–1.745)	0.006	1.441 (1.186–1.750)	0.004
One disease domain -> Death	High RC / high UHR	1.518 (1.079–2.134)	0.114	1.518 (1.079–2.135)	0.124
No disease domain -> One disease domain	High RC / low UHR	1.168 (1.017–1.341)	0.153	1.186 (1.029–1.366)	0.124

Cut-point sensitivity

When the cohort medians were used instead of the means, both principal associations remained in the same direction but had weaker multiplicity-adjusted evidence. The estimate for no disease domain to one disease domain was RRR 1.185 (95% CI 1.052–1.335; BH q = 0.140), and the estimate for one disease domain to multimorbidity was RRR 1.280 (95% CI 1.048–1.562; BH q = 0.207). The size and statistical certainty of the profile associations therefore depend in part on the sample-derived cut point.In the separate continuous model, RC showed modest associations with selected transitions, but the RC-by-UHR interaction was not clearly different from the null. The results of the alternative RC-handling and cut-point analyses for the two principal transitions are presented in Table 5.

Table 5
Sensitivity of the two principal transitions to RC handling and cut-point choice.

Transition	Mean cut point RRR (95% CI)	Mean BH q	RC > = 0 RRR (95% CI)	RC > = 0 BH q	Median cut point RRR (95% CI)	Median BH q
No disease domain -> One disease domain	1.245 (1.101–1.407)	0.006	1.258 (1.111–1.424)	0.004	1.185 (1.052–1.335)	0.140
One disease domain -> Multimorbidity	1.437 (1.184–1.745)	0.006	1.441 (1.186–1.750)	0.004	1.280 (1.048–1.562)	0.207

Supplementary exposure and robustness analyses

The continuous exposure analysis showed modest positive associations for RC with transition from no disease domain to one disease domain (RRR 1.063, 95% CI 1.000-1.131; P = 0.049), from no disease domain to multimorbidity (RRR 1.166, 95% CI 1.011–1.344; P = 0.034), and from one disease domain to

multimorbidity (RRR 1.114, 95% CI 1.014–1.223; P = 0.024). The corresponding RC-by-UHR interaction estimates were close to the null for no disease domain to one disease domain (RRR 0.988, 95% CI 0.961–1.016; P = 0.407) and one disease domain to multimorbidity (RRR 0.969, 95% CI 0.933–1.005; P = 0.093), providing no clear evidence of multiplicative interaction (Supplementary Table S5; Supplementary Figure S3).

Supplementary Tables S1-S3 and Supplementary Figures S1-S2 show the profile distribution and observed transition counts. The negative-RC sensitivity analysis preserved the two main high RC/high UHR associations, whereas the median-cutpoint analysis kept the same direction but not the BH-adjusted significance (Supplementary Table S6; Supplementary Figure S3). Together, these results support a stage-specific association while also showing that the categorical findings depend partly on how exposure groups are defined.

Predicted state occupancy

The model-predicted observed-state occupancy trajectories by joint RC/UHR profile are shown in Fig. 2. By 2020, the model predicted multimorbidity occupancy of 0.149 in the high RC/high UHR profile and 0.101 in the low RC/low UHR profile. The corresponding predicted death occupancies were 0.140 and 0.111.

Supplementary measurement-error sensitivity analysis

The supplementary HRS comparison is reported in Supplementary Table S7. Because its biomarker and disease-state definitions were not equivalent to those used in CHARLS, it was not incorporated into the primary Markov inference.

The constrained HMM log likelihood increased from − 26334.7 to -22769.4 over 30 EM iterations, but the prespecified stopping criterion was not reached. Estimated diagonal emission probabilities were 1.0000, 0.9997, and 0.9977 for the no-domain, one-domain, and multimorbidity states, respectively(Supplementary Table S8; Supplementary Figure S5). Supplementary Table S9 and Supplementary Figure S4 show the model-based 2020 occupancy estimates.

Discussion

The central finding was a stage-specific pattern. Compared with the low RC/low UHR profile, participants with high levels of both markers were more likely to move from no observed disease domain to a first domain and from one domain to multimorbidity. Both associations remained statistically significant after Benjamini-Hochberg adjustment and were almost identical after excluding participants with negative calculated RC values. The association with one-domain to death was directionally higher but did not remain significant after multiplicity correction, and estimates after established multimorbidity were less precise. The study therefore identifies where the joint metabolic profile appears most informative, rather than suggesting a uniform association across every transition.

The first innovation is conceptual and analytic: multimorbidity was modelled as a sequence of observable transitions rather than a yes/no endpoint. This separates the onset of a first disease domain from the later accumulation of multiple domains, showing that the same exposure profile can matter differently at different stages. The Markov framework also accommodates competing destinations, including apparent improvement and death, which gives a more faithful picture of how disease burden changes in a real ageing population [26–29].

The second innovation is the exposure strategy. RC and UHR summarize complementary metabolic signals: cholesterol carried in triglyceride-rich remnants, and the balance between uric acid and HDL cholesterol. Their joint classification therefore offers a practical way to describe metabolic heterogeneity beyond a single lipid measure. The outcome states bring cardiovascular, diabetes, and kidney domains into one cardiovascular-kidney-metabolic framework, with death included as an absorbing destination. Retaining reverse observed transitions also respects the fact that survey-based disease counts can change with diagnosis, treatment, reporting, and access to care rather than behaving like irreversible biological stages.

The concentration of associations in the early and intermediate transitions is clinically plausible. Before multimorbidity is established, metabolic abnormalities may help distinguish people who are beginning to accumulate disease domains. After multimorbidity develops, heterogeneity in disease combinations, treatment, severity, and survival may dilute a single baseline profile. This stage-specific pattern is precisely the type of information that a multi-state analysis can reveal and that a conventional single-endpoint model would miss.

The design provides several practical strengths. Five CHARLS waves supplied repeated observations, the models accounted for within-person clustering, and the 27 primary profile tests were evaluated with false-discovery-rate control. The principal associations were also checked using continuous exposures, exclusion of negative calculated RC values, and alternative median cut points. A separate HRS comparison is provided in Supplementary Table S7 so that external context is available without blending non-equivalent definitions into the primary model.

Several limitations define the scope of interpretation. RC and UHR were measured at baseline, disease states were based on observed rather than adjudicated diagnoses, and mortality was assigned by follow-up wave because exact death dates were unavailable. Complete-case models without survey weights may also affect representativeness and precision. These issues motivate, but do not negate, the main contribution: the present analysis is a longitudinal description of stage-specific associations in an ageing population, not a causal treatment study or a clinical threshold study.

Because HDL cholesterol contributes to both RC and UHR calculations, the high/high category may partly reflect shared mathematical information rather than biological synergy. The null continuous interaction is consistent with that cautious interpretation. Future work should examine the component biomarkers together, test nonlinear associations, and determine whether the joint profile improves prediction beyond established risk factors.

These observational associations should complement, not replace, established lipid-management and cardiovascular-prevention guidance [13–15].

The HRS comparison is reported in Supplementary Table S7 as supportive external context, not as a formal replication, because its exposure and outcome definitions were not equivalent to those in CHARLS. The constrained hidden Markov model likewise remains a secondary measurement-error analysis. Keeping these analyses separate preserves the interpretability of the primary CHARLS inference while making the additional evidence visible to readers.

The next step is to follow the profile over time. Repeated RC, uric acid, HDL cholesterol, and other metabolic measurements could distinguish persistent from transient risk. Disease-specific multi-state models may also show whether the profile is linked to different routes into multimorbidity, such as cardiovascular-first, diabetes-first, or kidney-first pathways. Independent cohorts with harmonized definitions will be important for testing transportability and for evaluating whether the profile adds predictive value beyond established risk factors.

Overall, the joint high RC/high UHR profile was associated with selected early and intermediate transitions in cardiovascular-diabetes-kidney disease burden. The study's distinctive contribution is to show where this association appears along the multimorbidity pathway, using a transparent multi-state framework; the HRS comparison is retained separately as supportive context. The findings support further research on stage-specific metabolic risk and prevention in ageing populations.

Conclusions

In this longitudinal CHARLS analysis, the joint high RC/high UHR profile was associated with two clinically important steps in disease accumulation: entry from no observed disease domain into a first cardiovascular, diabetes, or kidney domain, and progression from one domain to multimorbidity. Both associations survived correction for multiple comparisons and were essentially unchanged after excluding participants with negative calculated RC values. The principal contribution of the study is the combination of complementary metabolic markers with a stage-specific multi-state model, which identifies where risk is concentrated rather than treating multimorbidity as an undifferentiated endpoint. The HRS comparison is reported separately as supportive context because its definitions were not equivalent to those used in CHARLS. These findings provide a focused basis for future work on longitudinal metabolic profiles, disease-specific pathways, and prevention strategies.

Declarations

Funding sources: This work was supported by the National Science Foundation of China (No. 81773312); Social Development Science and Technology Project of Dongguan (No. 20221800906082 No. 20231800936282 No. 20221800906092).

Ethical approval: Not applicable.

Clinical trial number: Not applicable.

Consent for publication: Not applicable.

Competing interests: No financial or non-financial benefits have been received or will be received from any party related directly or indirectly to the subject of this article.

Authors' contributions: Conception and design: HW. Data collection and interpretation: HW, YW, YL, JQ. Statistical analysis: HW, YW, LL. Writing original draft: YW, HW, YL, JQ, and XX. Writing review and editing: HW, YW, YL, JQ, LL, YP, XX, QL, SL and CL. Supervision: YH. Final approval of manuscript: all authors.

Acknowledgments: We appreciate the valuable contributions of the participants and staff of the CHARLS database.

Data Availability: The data analyzed in this study were obtained from the China Health and Retirement Longitudinal Study (CHARLS) and, for the supplementary external comparison, the Health and Retirement Study (HRS). CHARLS data and related documentation are available to registered users through the official CHARLS website. HRS public-release data can be accessed after registration through the official HRS Data Products portal, subject to the study's data-use conditions.

References

1. Ndumele CE, Rangaswami J, Chow SL, et al. Cardiovascular-Kidney-Metabolic Health: A Presidential Advisory From the American Heart Association. Circulation. 2023;148:1606–36. 10.1161/CIR.0000000000001186.
2. Zhao Y, Hu Y, Smith JP, Strauss J, Yang G. Cohort profile: the China Health and Retirement Longitudinal Study (CHARLS). Int J Epidemiol. 2014;43:61–8. 10.1093/ije/dys203.
3. Sonnega A, Faul JD, Ofstedal MB, Langa KM, Phillips JWR, Weir DR. Cohort profile: the Health and Retirement Study (HRS). Int J Epidemiol. 2014;43:576–85. 10.1093/ije/dyu067.
4. Barnett K, Mercer SW, Norbury M, Watt G, Wyke S, Guthrie B. Epidemiology of multimorbidity and implications for health care, research, and medical education: a cross-sectional study. Lancet. 2012;380:37–43. 10.1016/S0140-6736(12)60240-2.
5. Tinetti ME, Fried TR, Boyd CM. Designing health care for the most common chronic condition-multimorbidity. JAMA. 2012;307:2493–4. 10.1001/jama.2012.5265.
6. Roth GA, Mensah GA, Johnson CO, et al. Global burden of cardiovascular diseases and risk factors, 1990–2019: update from the GBD 2019 study. J Am Coll Cardiol. 2020;76:2982–3021. 10.1016/j.jacc.2020.11.010.
7. GBD 2019 Diseases and Injuries Collaborators. Global burden of 369 diseases and injuries in 204 countries and territories, 1990–2019: a systematic analysis for the Global Burden of Disease Study 2019. Lancet. 2020;396:1204–22. 10.1016/S0140-6736(20)30925-9.

8. GBD 2019 Risk Factors Collaborators. Global burden of 87 risk factors in 204 countries and territories, 1990–2019: a systematic analysis for the Global Burden of Disease Study 2019. Lancet. 2020;396:1223–49. 10.1016/S0140-6736(20)30752-2.
9. Varbo A, Benn M, Tybjaerg-Hansen A, Jorgensen AB, Frikke-Schmidt R, Nordestgaard BG. Remnant cholesterol as a causal risk factor for ischemic heart disease. J Am Coll Cardiol. 2013;61:427–36. 10.1016/j.jacc.2012.08.1026.
10. Nordestgaard BG, Varbo A. Triglyceride-rich lipoproteins and cardiovascular disease. Lancet. 2014;384:626–35. 10.1016/S0140-6736(14)60577-6.
11. Castaner O, Pinto X, Subirana I, et al. Remnant cholesterol, not LDL cholesterol, is associated with incident coronary heart disease. J Am Coll Cardiol. 2020;76:2712–24. 10.1016/j.jacc.2020.10.008.
12. Ference BA, Ginsberg HN, Graham I, et al. Low-density lipoproteins cause atherosclerotic cardiovascular disease. 1. Evidence from genetic, epidemiologic, and clinical studies. Eur Heart J. 2017;38:2459–72. 10.1093/eurheartj/ehx144.
13. Grundy SM, Stone NJ, Bailey AL, AHA/ACC/AACVPR/AAPA/ABC et al. /ACPM/ADA/AGS/APhA/ASPC/NLA/PCNA guideline on the management of blood cholesterol. Circulation. 2019;139:e1082-e1143. 10.1161/CIR.0000000000000625
14. Arnett DK, Blumenthal RS, Albert MA, et al. 2019 ACC/AHA guideline on the primary prevention of cardiovascular disease. Circulation. 2019;140:e596–646. 10.1161/CIR.0000000000000678.
15. Visseren FLJ, Mach F, Smulders YM, et al. 2021 ESC Guidelines on cardiovascular disease prevention in clinical practice. Eur Heart J. 2021;42:3227–337. 10.1093/eurheartj/ehab484.
16. Johnson RJ, Kang DH, Feig D, et al. Is there a pathogenetic role for uric acid in hypertension and cardiovascular and renal disease? Hypertension. 2003;41:1183–90. 10.1161/01.HYP.0000069700.62727.C5.
17. Feig DI, Kang DH, Johnson RJ. Uric acid and cardiovascular risk. N Engl J Med. 2008;359:1811–21. 10.1056/NEJMra0800885.
18. Borghi C, Agabiti-Rosei E, Johnson RJ, et al. Hyperuricaemia and cardiovascular disease risk. Expert Rev Cardiovasc Ther. 2015;13:1219–31. 10.1586/14779072.2015.1087123.
19. Aktas G, Kocak MZ, Bilgin S, et al. Uric acid to HDL cholesterol ratio is a strong predictor of metabolic syndrome. Clin Appl Thromb Hemost. 2020;26:1076029620969149. 10.1177/1076029620969149.
20. Cheng Y, et al. Association of serum uric acid to HDL cholesterol ratio with chronic kidney disease: a cross-sectional study. BMJ Open. 2022;12:e066243. 10.1136/bmjopen-2022-066243.
21. Yu H, et al. The association between uric acid-to-HDL cholesterol ratio and metabolic syndrome: a population-based study. Postgrad Med. 2024;136:58–66. 10.1080/00325481.2023.2263372.
22. Lai X, Chen T. Association of serum uric acid to high-density lipoprotein cholesterol ratio with all-cause and cardiovascular mortality in patients with diabetes or prediabetes: a prospective cohort study. Front Endocrinol (Lausanne). 2024;15:1476336. 10.3389/fendo.2024.1476336.

23. Yi Y, Luo Q, Chen J, et al. Association between the uric acid-to-HDL-cholesterol ratio and the risk of cardiovascular disease and dyslipidemia: a population-based study. Lipids Health Dis. 2025;24:143. 10.1186/s12944-025-02551-4.
24. Go AS, Chertow GM, Fan D, McCulloch CE, Hsu CY. Chronic kidney disease and the risks of death, cardiovascular events, and hospitalization. N Engl J Med. 2004;351:1296–305. 10.1056/NEJMoa041031.
25. Matsushita K, van der Velde M, Astor BC, et al. Association of estimated glomerular filtration rate and albuminuria with all-cause and cardiovascular mortality in general population cohorts: a collaborative meta-analysis. Lancet. 2010;375:2073–81. 10.1016/S0140-6736(10)60674-5.
26. Putter H, Fiocco M, Geskus RB. Tutorial in biostatistics: competing risks and multi-state models. Stat Med. 2007;26:2389–430. 10.1002/sim.2712.
27. Andersen PK, Keiding N. Multi-state models for event history analysis. Stat Methods Med Res. 2002;11:91–115. 10.1191/0962280202sm276ra.
28. Hougaard P. Multi-state models: a review. Lifetime Data Anal. 1999;5:239–64. 10.1023/A:1009672031538.
29. Aalen OO, Borgan O, Gjessing HK. Survival and Event History Analysis: A Process Point of View. New York: Springer; 2008.
30. Zucchini W, MacDonald IL, Langrock R. Hidden Markov Models for Time Series: An Introduction Using R. 2nd ed. Boca Raton: Chapman and Hall/CRC; 2017.
31. Jackson CH. Multi-state models for panel data: the msm package for R. J Stat Softw. 2011;38(8):1–28. 10.18637/jss.v038.i08.
32. von Elm E, Altman DG, Egger M, et al. The Strengthening the Reporting of Observational Studies in Epidemiology (STROBE) statement: guidelines for reporting observational studies. PLoS Med. 2007;4:e296. 10.1371/journal.pmed.0040296.
33. Sterne JAC, White IR, Carlin JB, et al. Multiple imputation for missing data in epidemiological and clinical research: potential and pitfalls. BMJ. 2009;338:b2393. 10.1136/bmj.b2393.
34. White IR, Royston P, Wood AM. Multiple imputation using chained equations: issues and guidance for practice. Stat Med. 2011;30:377–99. 10.1002/sim.4067.
35. Little RJ, D'Agostino R, Cohen ML, et al. The prevention and treatment of missing data in clinical trials. N Engl J Med. 2012;367:1355–60. 10.1056/NEJMsr1203730.
36. VanderWeele TJ, Ding P. Sensitivity analysis in observational research: introducing the E-value. Ann Intern Med. 2017;167:268–74. 10.7326/M16-2607.
37. Rubin DB. Multiple Imputation for Nonresponse in Surveys. New York: Wiley; 1987.
38. Hernan MA, Robins JM. Causal Inference: What If. Boca Raton: Chapman & Hall/CRC; 2020.

Figures

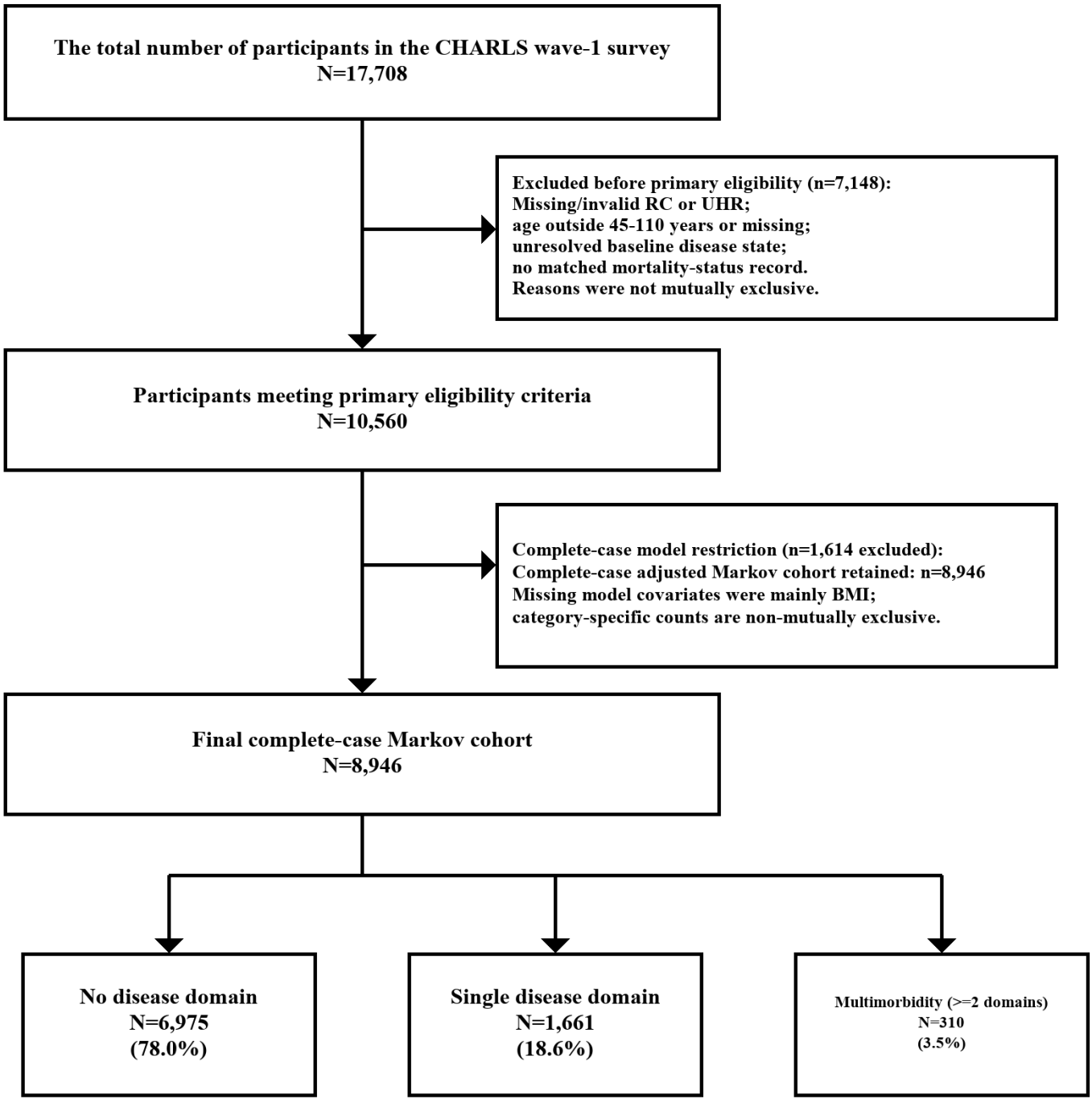


Figure 1

Participant Selection Flowchart

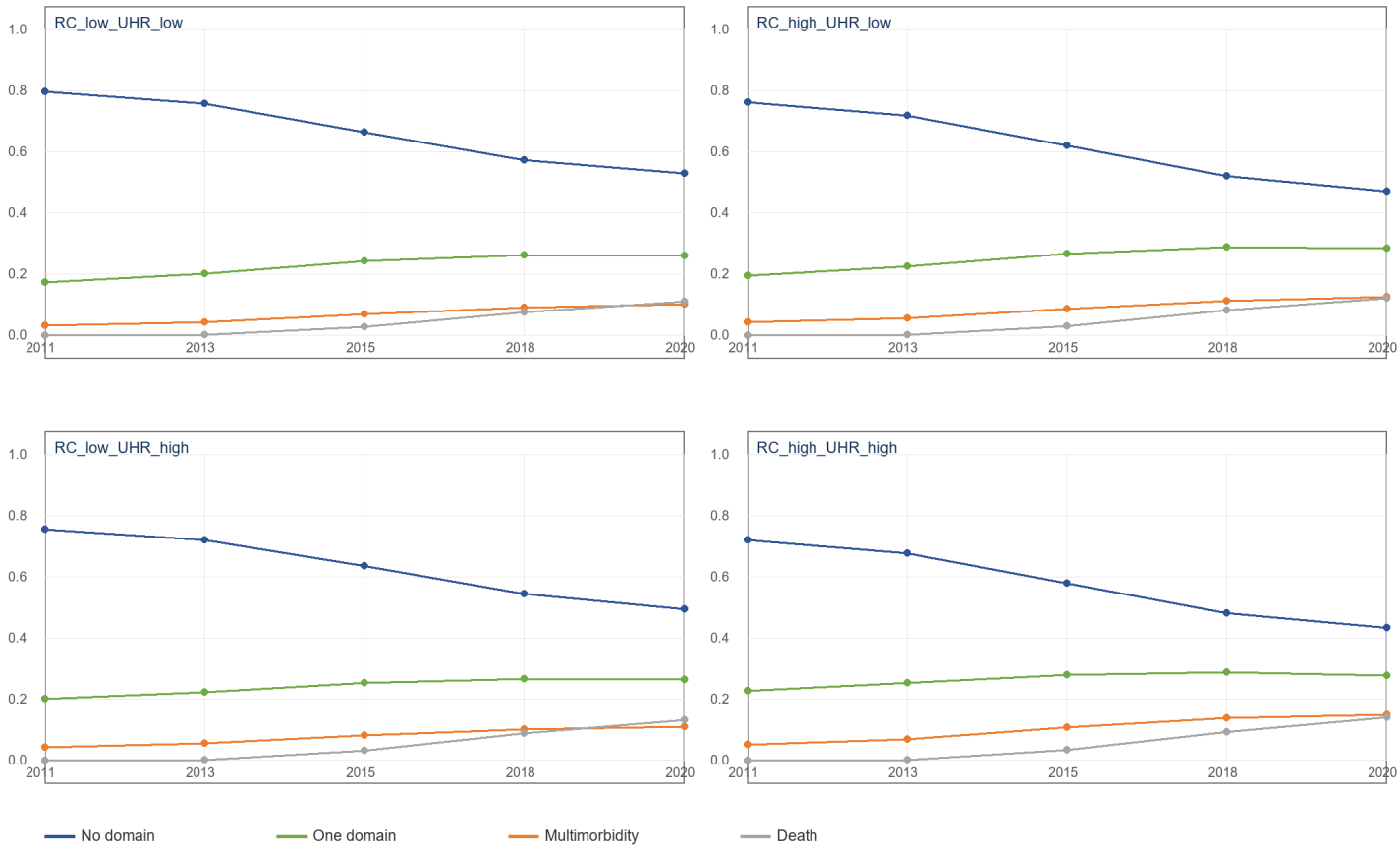


Figure 2

Model-predicted observed-state occupancy trajectories by joint RC/UHR profile.

Supplementary Files

This is a list of supplementary files associated with this preprint. Click to download.

- Supplementary.docx